The many elements to the article of the future

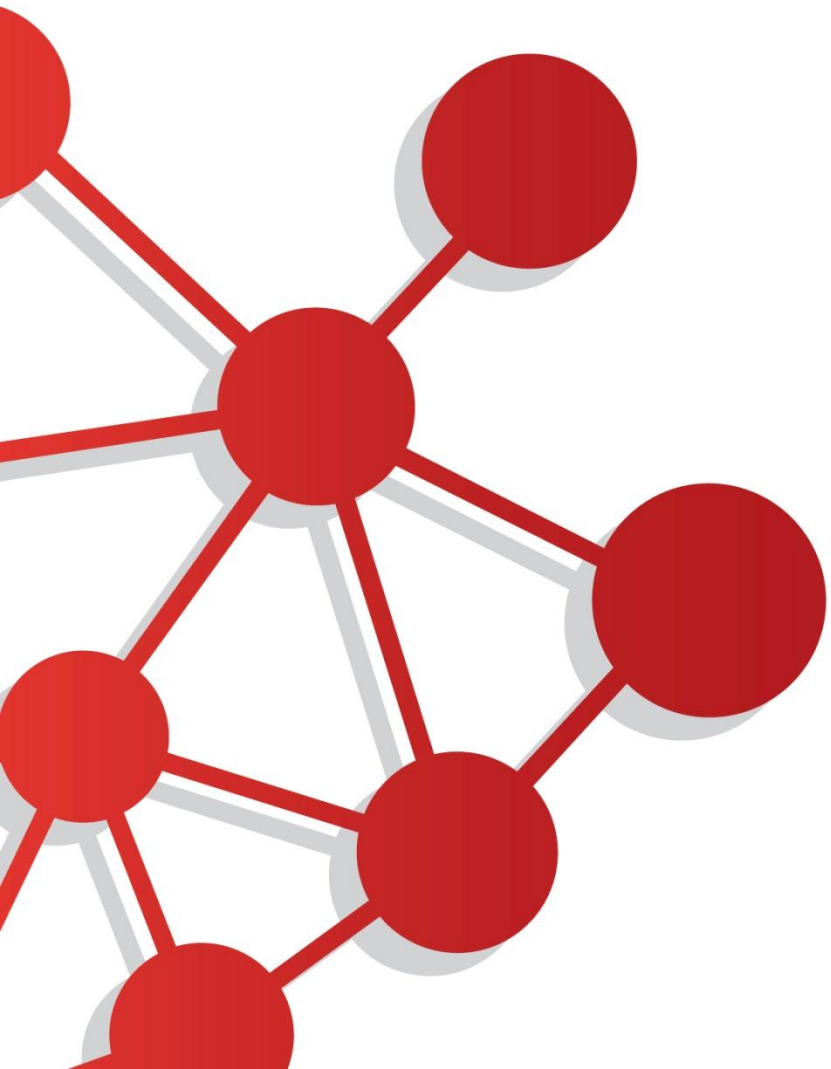

Jason Wilde
Nature Publishing Group
15th October 2012

nature publishing group npg

Article of the future…

- Evolution of research
- Publishing technology
- Beyond [the] paper
- External data/information
- Text, data, metadata
- The article of the future…
- The end..?

Evolution of research

MOLECULAR STRUCTURE OF NUCLEIC ACIDS

A Structure for Deoxyribose Nucleic Acid

DNA Structure 1953

1 Page

2 Authors

1 Figure

no data

Evolution of research

Human Genome 2001

62 Pages, 150 Authors,

49 Figure, 27 tables


articles

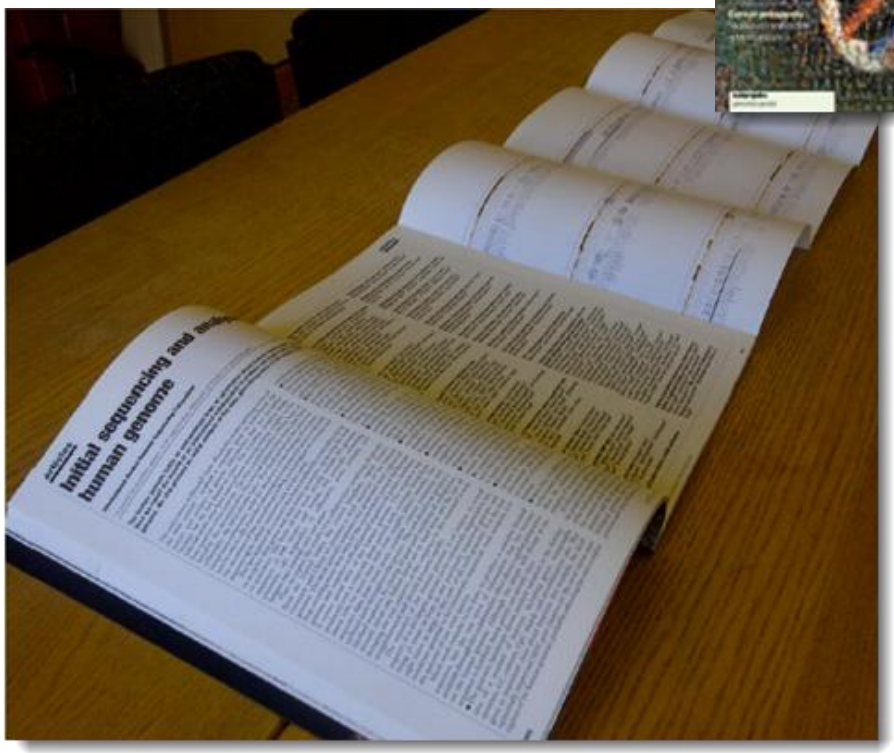

Evolution of research

1000 Genome Project 2010

12 page, 76 Institutions, 12,145 SRA run ids

Evolution of research

Encode Project 2012

30 papers, 3 Journals

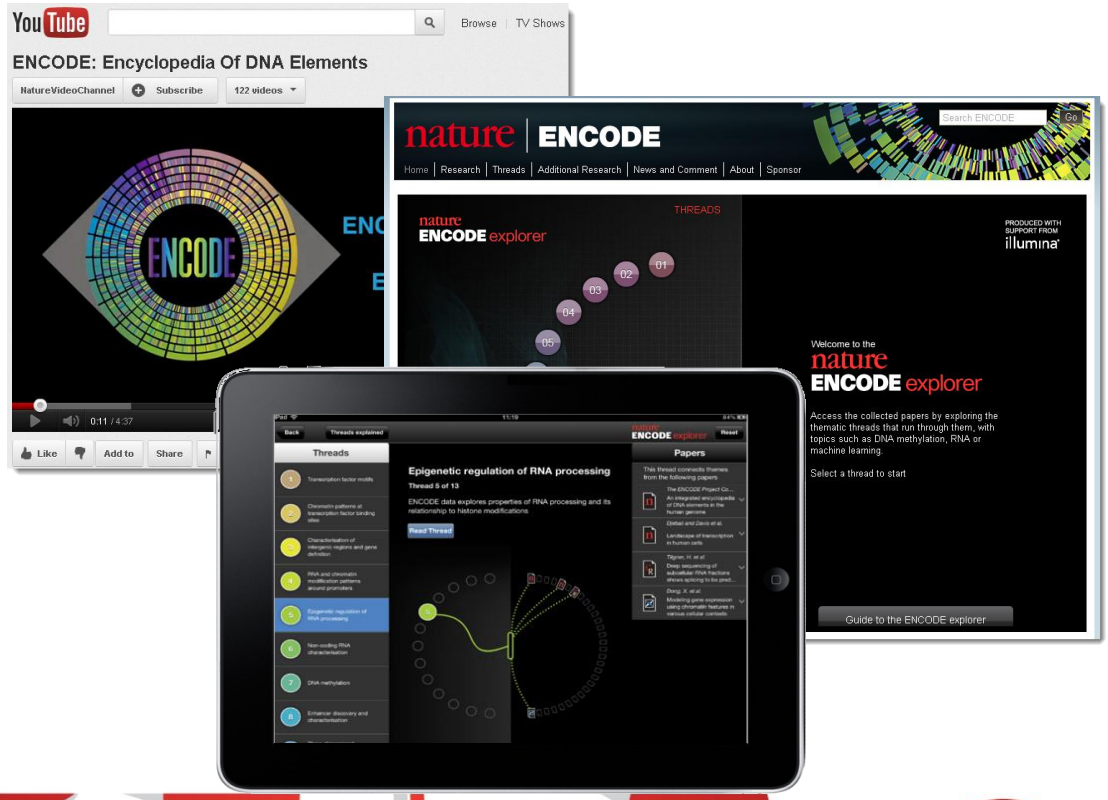

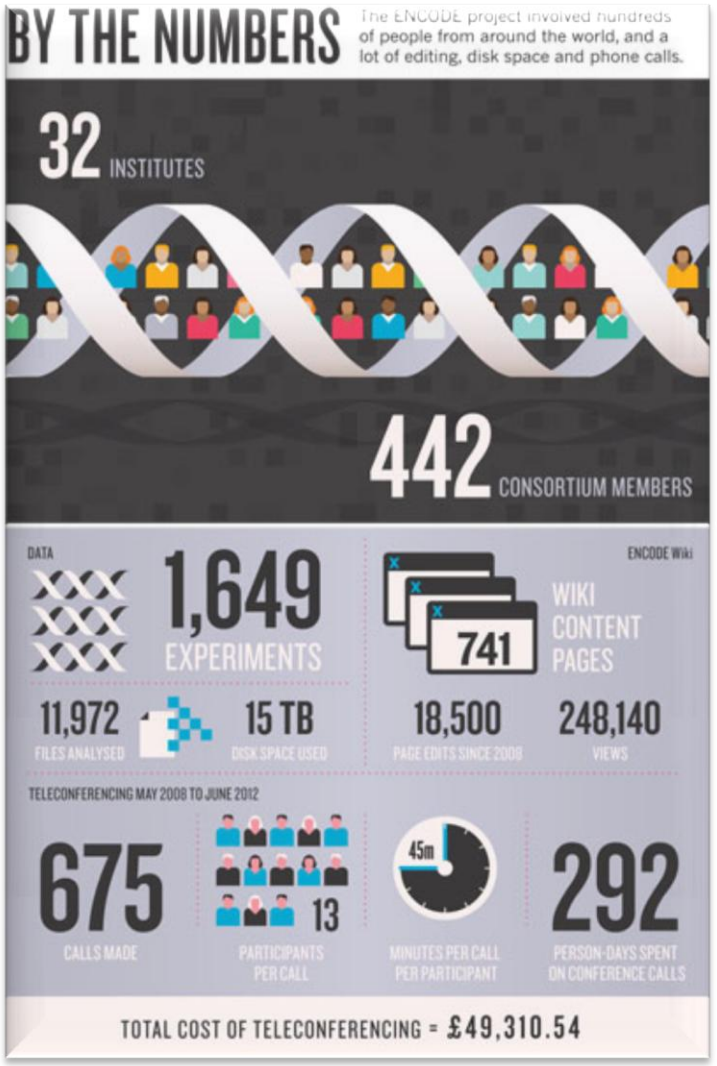

nature publishing group npg

Evolution of research

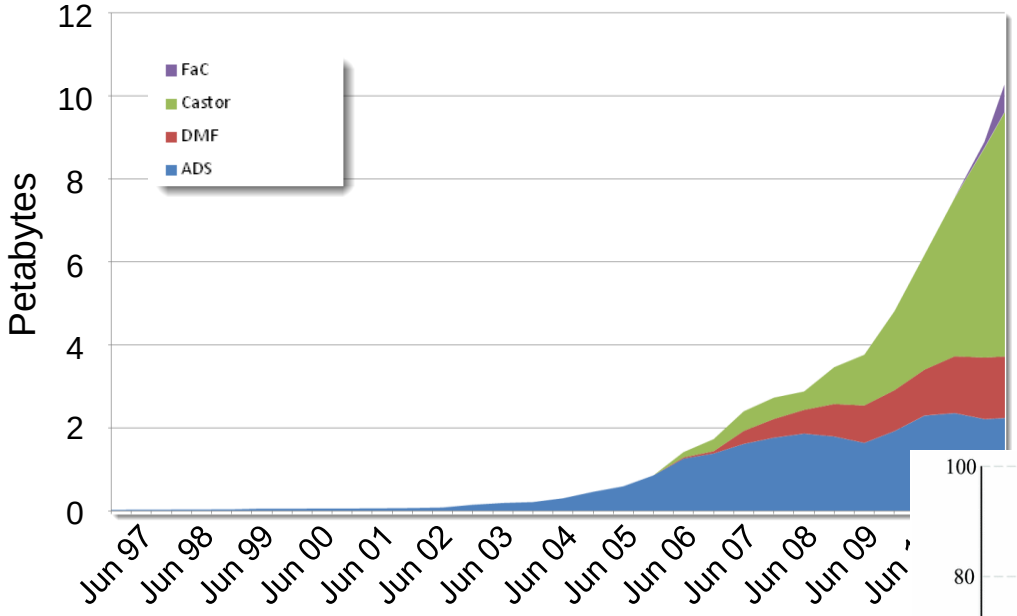

- **CERN** high energy physics data from the Atlas, LHCb, CMS and Alice. These data are stored using the CERN designed **Castor** infrastructure
- **Castor** is also used to store data from STFC's UK facilities (**FaC**).
- **ADS** is the old archive with lots of small backups.
- **DMF** includes the preserved documents from the CEDA Repository at the British Atmospheric Data Centre, and Tesella Safety Deposit Box (SDB) services to preserve data collected on the ISIS, Diamond and CLF facilities.

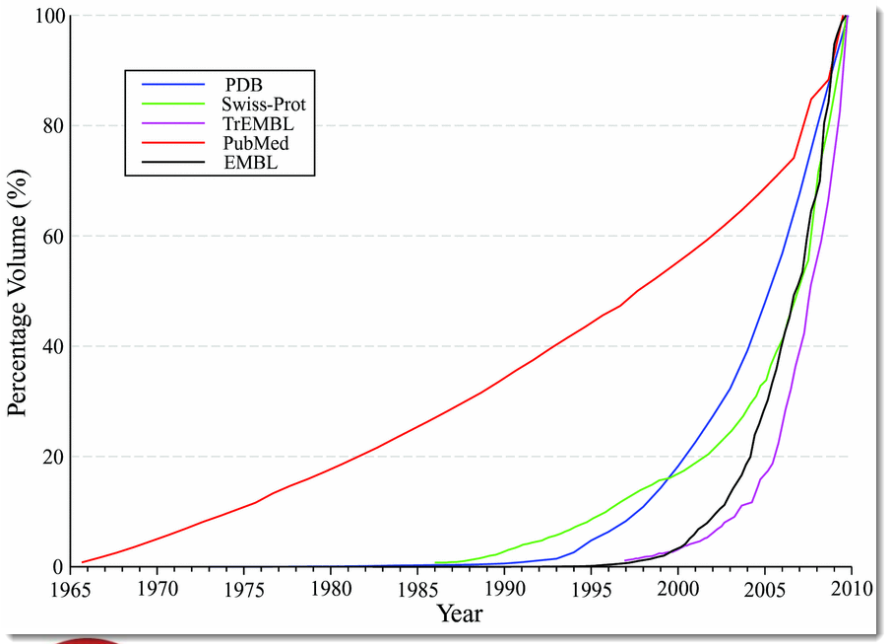

Graphical illustration of the growth of biomedical research publications (**red**; current total >19 million), alongside the accumulation of research data, including nucleic acid sequences (**black**; current total ~163 million), computer-annotated protein sequences (**magenta**; current total 9 million), manually annotated protein sequences (**green**; current total 500000) and protein structures (**blue**; current total 60000)

Publishing technology

It used to be so very simple…

Publishing technology

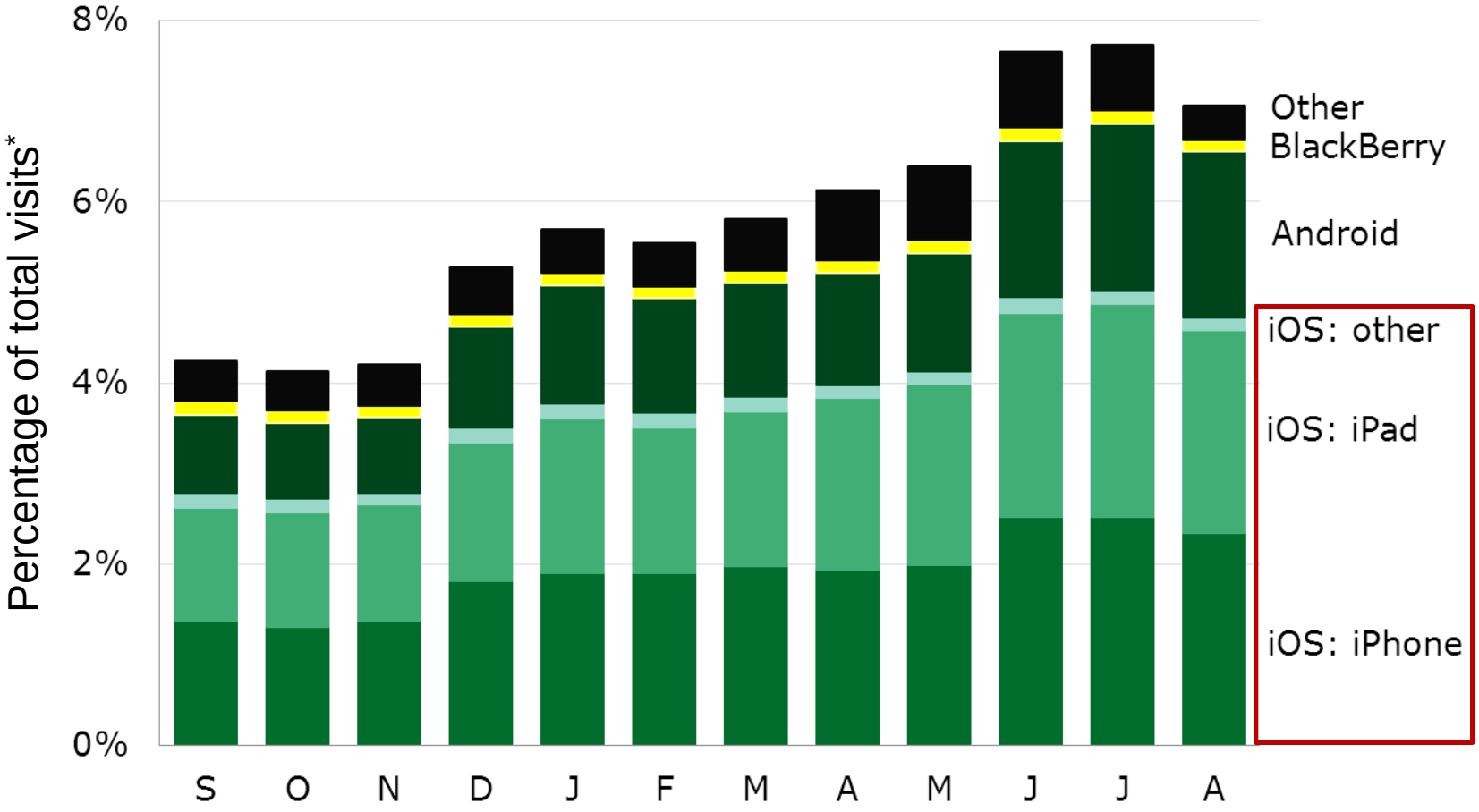

* % based on *ca* 13.5M visit per month

Beyond [the] paper

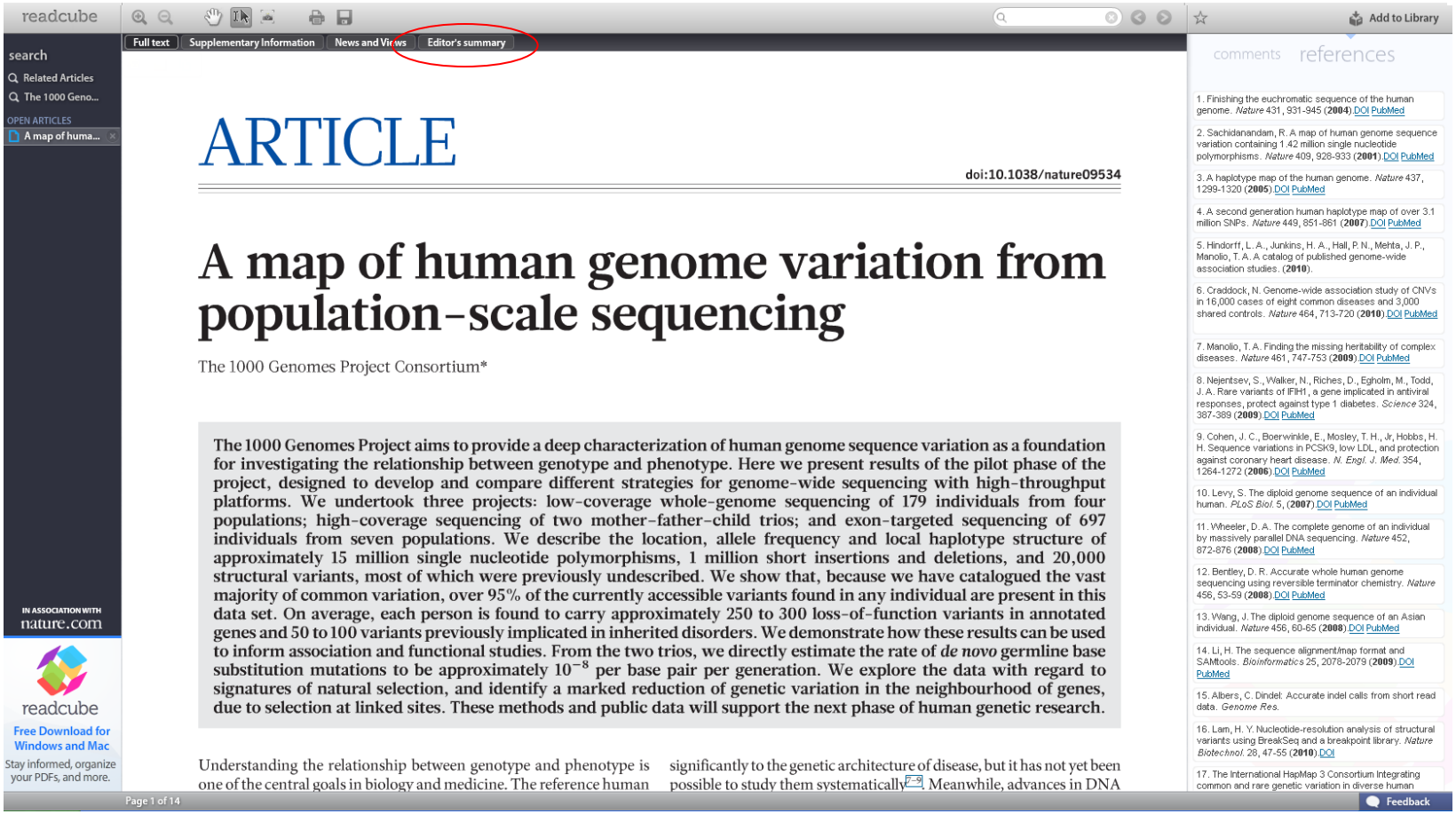

Beyond [the] paper

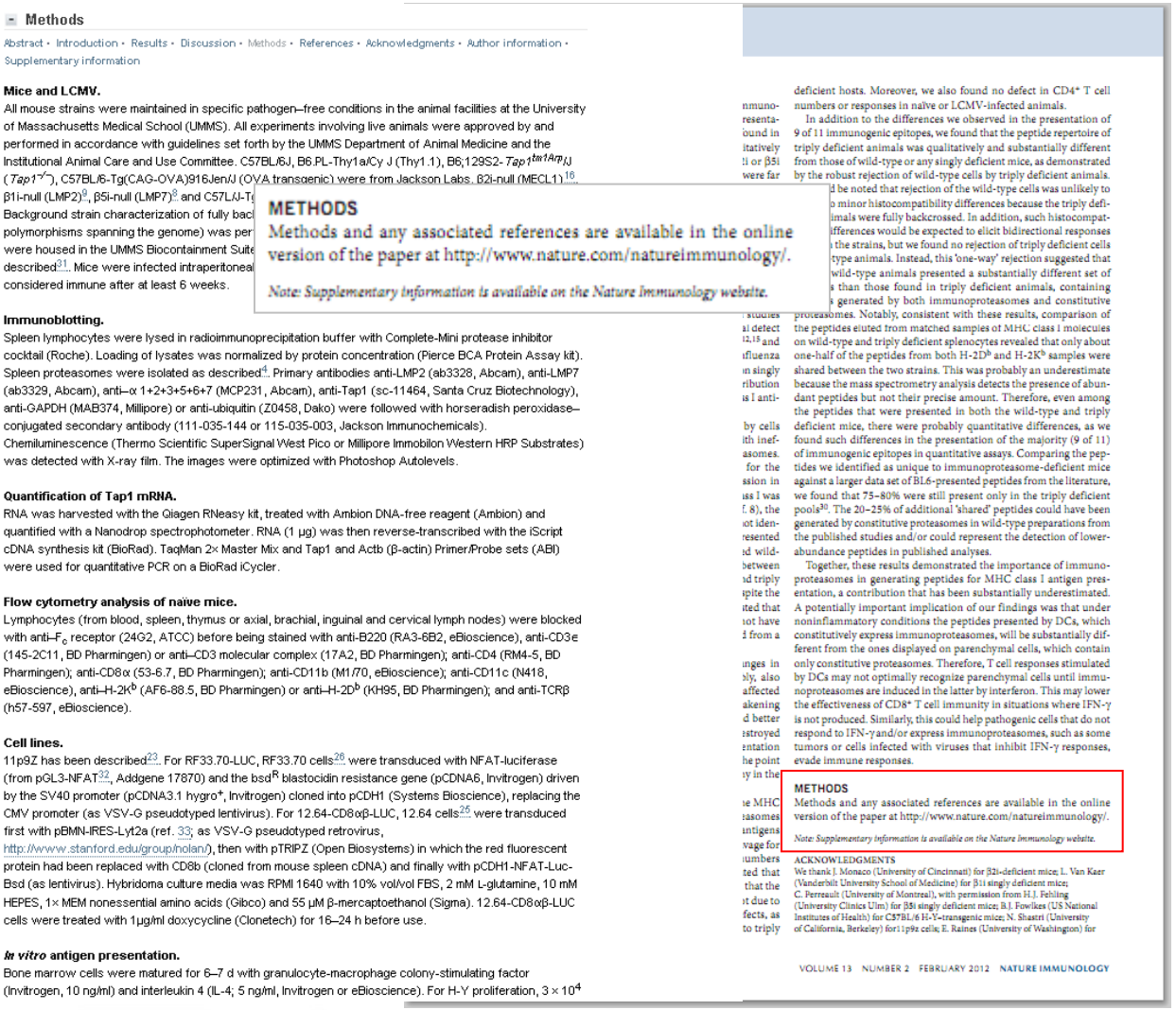

Methods

Mice and LCMV.
All mouse strains were maintained in specific pathogen–free conditions in the animal facilities at the University of Massachusetts Medical School (UMMS). All experiments involving live animals were approved by and performed in accordance with guidelines set forth by the UMMS Department of Animal Medicine and the Institutional Animal Care and Use Committee. C57BL/6J, B6.PL-Thy1a/Cy J (Thy1.1), B6;129S2-*Tap1*^{tm1Arp}/J (*Tap1*$^{-/-}$), C57BL/6-Tg(CAG-OVA)916Jen/J (OVA transgenic) were from Jackson Labs. β2i-null (MECL1)[16], β1i-null (LMP2)[9], β5i-null (LMP7)[8] and C57L/J-T
Background strain characterization of fully bac
polymorphisms spanning the genome) was per
were housed in the UMMS Biocontainment Suite
described[31]. Mice were infected intraperitonea
considered immune after at least 6 weeks.

Immunoblotting.
Spleen lymphocytes were lysed in radioimmunoprecipitation buffer with Complete-Mini protease inhibitor cocktail (Roche). Loading of lysates was normalized by protein concentration (Pierce BCA Protein Assay kit). Spleen proteasomes were isolated as described[4]. Primary antibodies anti-LMP2 (ab3328, Abcam), anti-LMP7 (ab3329, Abcam), anti–α 1+2+3+5+6+7 (MCP231, Abcam), anti-Tap1 (sc-11464, Santa Cruz Biotechnology), anti-GAPDH (MAB374, Millipore) or anti-ubiquitin (Z0458, Dako) were followed with horseradish peroxidase–conjugated secondary antibody (111-035-144 or 115-035-003, Jackson Immunochemicals). Chemiluminescence (Thermo Scientific SuperSignal West Pico or Millipore Immobilon Western HRP Substrates) was detected with X-ray film. The images were optimized with Photoshop Autolevels.

Quantification of Tap1 mRNA.
RNA was harvested with the Qiagen RNeasy kit, treated with Ambion DNA-free reagent (Ambion) and quantified with a Nanodrop spectrophotometer. RNA (1 μg) was then reverse-transcribed with the iScript cDNA synthesis kit (BioRad). TaqMan 2× Master Mix and Tap1 and Actb (β-actin) Primer/Probe sets (ABI) were used for quantitative PCR on a BioRad iCycler.

Flow cytometry analysis of naive mice.
Lymphocytes (from blood, spleen, thymus or axial, brachial, inguinal and cervical lymph nodes) were blocked with anti–F_c receptor (24G2, ATCC) before being stained with anti-B220 (RA3-6B2, eBioscience), anti-CD3ε (145-2C11, BD Pharmingen) or anti–CD3 molecular complex (17A2, BD Pharmingen); anti-CD4 (RM4-5, BD Pharmingen); anti-CD8α (53-6.7, BD Pharmingen); anti-CD11b (M1/70, eBioscience); anti-CD11c (N418, eBioscience), anti–H-2K^b (AF6-88.5, BD Pharmingen) or anti–H-2D^b (KH95, BD Pharmingen); and anti-TCRβ (h57-597, eBioscience).

Cell lines.
11p9Z has been described[23]. For RF33.70-LUC, RF33.70 cells[26] were transduced with NFAT-luciferase (from pGL3-NFAT[32], Addgene 17870) and the bsd^R blastocidin resistance gene (pCDNA6, Invitrogen) driven by the SV40 promoter (pCDNA3.1 hygro$^+$, Invitrogen) cloned into pCDH1 (Systems Bioscience), replacing the CMV promoter (as VSV-G pseudotyped lentivirus). For 12.64-CD8αβ-LUC, 12.64 cells[25] were transduced first with pBMN-IRES-Lyt2a (ref. 33; as VSV-G pseudotyped retrovirus, http://www.stanford.edu/group/nolan/), then with pTRIPZ (Open Biosystems) in which the red fluorescent protein had been replaced with CD8b (cloned from mouse spleen cDNA) and finally with pCDH1-NFAT-Luc-Bsd (as lentivirus). Hybridoma culture media was RPMI 1640 with 10% vol/vol FBS, 2 mM L-glutamine, 10 mM HEPES, 1× MEM nonessential amino acids (Gibco) and 55 μM β-mercaptoethanol (Sigma). 12.64-CD8αβ-LUC cells were treated with 1μg/ml doxycycline (Clonetech) for 16–24 h before use.

***In vitro* antigen presentation.**
Bone marrow cells were matured for 6–7 d with granulocyte-macrophage colony-stimulating factor (Invitrogen, 10 ng/ml) and interleukin 4 (IL-4; 5 ng/ml, Invitrogen or eBioscience). For H-Y proliferation, 3×10^4

METHODS
Methods and any associated references are available in the online version of the paper at http://www.nature.com/natureimmunology/.
Note: Supplementary Information is available on the Nature Immunology website.

deficient hosts. Moreover, we also found no defect in CD4$^+$ T cell numbers or responses in naïve or LCMV-infected animals.

In addition to the differences we observed in the presentation of 9 of 11 immunogenic epitopes, we found that the peptide repertoire of triply deficient animals was qualitatively and substantially different from those of wild-type or any singly deficient mice, as demonstrated by the robust rejection of wild-type cells by triply deficient animals. d be noted that rejection of the wild-type cells was unlikely to o minor histocompatibility differences because the triply defi- imals were fully backcrossed. In addition, such histocompat- ifferences would be expected to elicit bidirectional responses the strains, but we found no rejection of triply deficient cells type animals. Instead, this 'one-way' rejection suggested that wild-type animals presented a substantially different set of s than those found in triply deficient animals, containing s generated by both immunoproteasomes and constitutive proteasomes. Notably, consistent with these results, comparison of the peptides eluted from matched samples of MHC class I molecules on wild-type and triply deficient splenocytes revealed that only about one-half of the peptides from both H-2D^b and H-2K^b samples were shared between the two strains. This was probably an underestimate because the mass spectrometry analysis detects the presence of abundant peptides but not their precise amount. Therefore, even among the peptides that were presented in both the wild-type and triply deficient mice, there were probably quantitative differences, as we found such differences in the presentation of the majority (9 of 11) of immunogenic epitopes in quantitative assays. Comparing the peptides we identified as unique to immunoproteasome-deficient mice against a larger data set of BL6-presented peptides from the literature, we found that 75–80% were still present only in the triply deficient pools[30]. The 20–25% of additional 'shared' peptides could have been generated by constitutive proteasomes in wild-type preparations from the published studies and/or could represent the detection of lower-abundance peptides in published analyses.

Together, these results demonstrated the importance of immunoproteasomes in generating peptides for MHC class I antigen presentation, a contribution that has been substantially underestimated. A potentially important implication of our findings was that under noninflammatory conditions the peptides presented by DCs, which constitutively express immunoproteasomes, will be substantially different from the ones displayed on parenchymal cells, which contain only constitutive proteasomes. Therefore, T cell responses stimulated by DCs may not optimally recognize parenchymal cells until immunoproteasomes are induced in the latter by interferon. This may lower the effectiveness of CD8$^+$ T cell immunity in situations where IFN-γ is not produced. Similarly, this could help pathogenic cells that do not respond to IFN-γ and/or express immunoproteasomes, such as some tumors or cells infected with viruses that inhibit IFN-γ responses, evade immune responses.

METHODS
Methods and any associated references are available in the online version of the paper at http://www.nature.com/natureimmunology/.
Note: Supplementary Information is available on the Nature Immunology website.

ACKNOWLEDGMENTS
We thank J. Monaco (University of Cincinnati) for β2i-deficient mice; L. Van Kaer (Vanderbilt University School of Medicine) for β1i singly deficient mice; C. Perreault (University of Montreal), with permission from H.J. Fehling (University Clinics Ulm) for β5i singly deficient mice; B.J. Fowlkes (US National Institutes of Health) for C57BL/6 H-Y–transgenic mice; N. Shastri (University of California, Berkeley) for 11p9z cells; E. Raines (University of Washington) for

Beyond [the] paper

PROTOCOL

Assay of protein kinases using a protocol

C James Hastie[1,3], Hilary J McLauchlan[1,3] & Philip Cohen[2]

[1]Division of Signal Transduction Therapy and [2]Medical Research Council Protein Phosphorylation Unit, University of Dundee, Dow Street, Dundee DD1 5EH, Scotland. [3]These authors contributed equally. P.C. (p.cohen@dundee.ac.uk).

Published online 3 August 2006; doi:10.1038/nprot.2006.149

Protein kinase activity results in the incorporation of radiolabeled phosphate The measurement of the amount of radioactivity incorporated into a substrate enzyme activity to be quantified. The activity is expressed as a 'unit', where 1 catalyzes the incorporation of 1 nanomole of phosphate into the standard sub of activity per milligram protein. The assay format described here is quick, sim direct measurement of activity and remains the 'gold standard' for the quantifi be assayed manually at one time, and the assay takes one person less than 1

INTRODUCTION

The attachment and removal of phosphate from proteins, called 'reversible phosphorylation', is catalyzed by two classes of enzyme, called 'protein kinases' and 'protein phosphatases'. Protein phosphorylation regulates nearly all aspects of cell life, and protein kinases are the largest single family of enzymes encoded by the human genome, with over 500 members. Abnormal protein phosphorylation is a cause or a consequence of major diseases worldwide, including cancer, diabetes and chronic inflammatory diseases. For that reason, protein kinases have become the second most highly studied class of drug target, behind G protein–coupled receptors (GPCRs), and are a chief area of research for both academic laboratories and the pharmaceutical industry[1]. Protein kinases catalyze the phosphorylation of serine, threonine, tyrosine and histidine residues on their target proteins, a reaction that involves the transfer of the γ-phosphoryl group of ATP to the amino acid side chain according to the following chemical equation: Mg-ATP + protein + protein kinase → phosphorylated protein + Mg-ADP + protein kinase.

Protein kinase activity is measured most conveniently using radiolabeled [γ-^{32}P]ATP and an appropriate acceptor peptide or protein substrate. The assay method described here was initially developed in the late 1970s and involves the use of phosphocellulose paper squares to capture the phosphorylated peptides or proteins resulting from the protein kinase reaction[2,3]. The papers are immersed in phosphoric acid to convert the acceptor peptides and proteins to positively charged species, which bind quantitatively to the negatively charged phosphocellulose paper[4]. The papers are washed extensively in phosphoric acid to remove all the [γ-^{32}P]ATP substrate included in the assay. ATP, being negatively charged, does not adhere to the phosphocellulose papers and is washed away, leaving only radiolabeled product bound to the papers, which can then be measured.

This method can be used to study the phosphorylation of all proteins that are phosphorylated on serine, threonine and tyrosine residues, except the extremely few proteins that would not be positively charged at a pH of 1.8. Small peptide substrates should have a charge of at least +2 (and ideally +3) at a pH of 1.8 to bind

nature publishing group npg

Beyond [the] paper

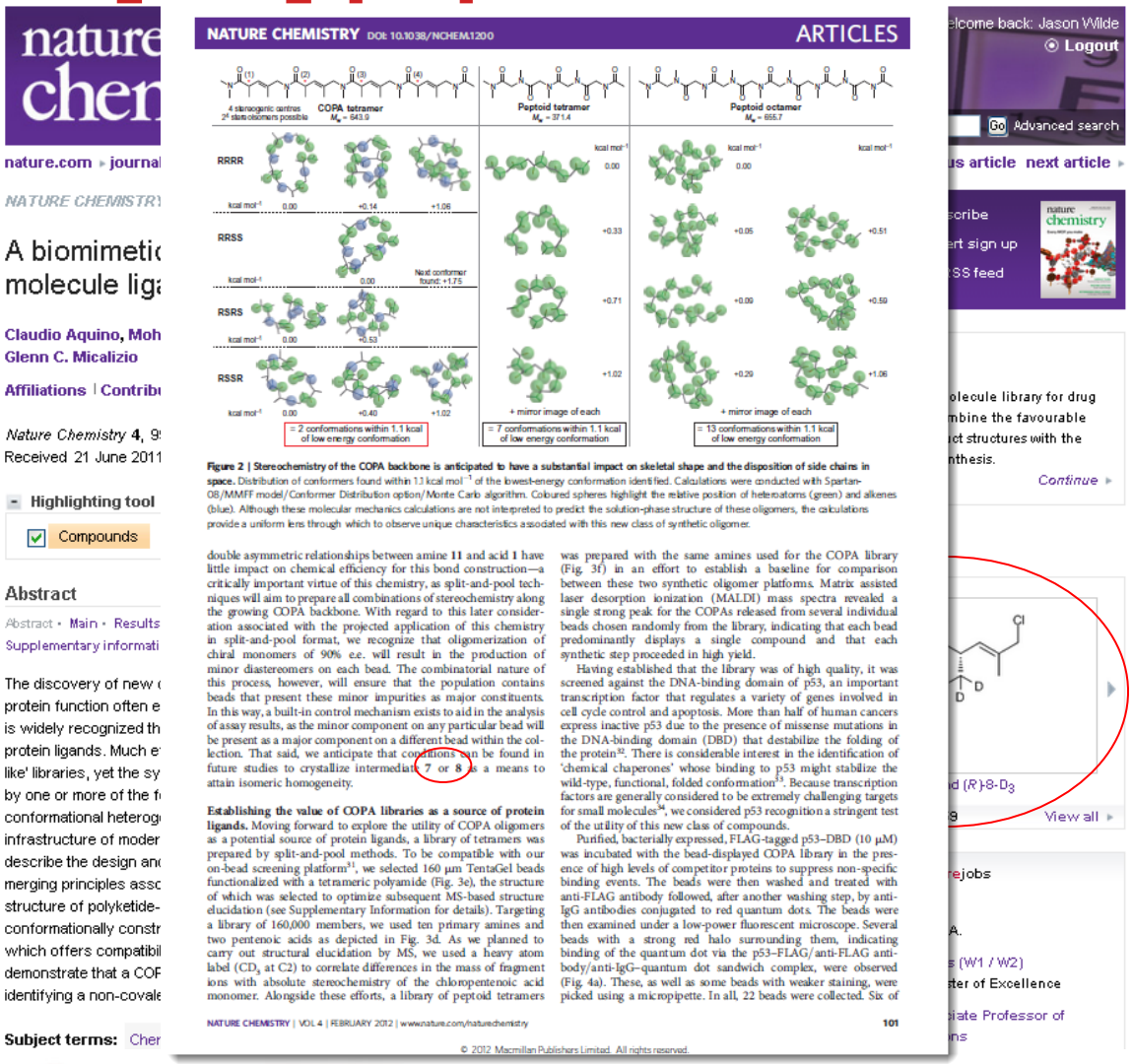

nature chem

nature.com ▸ journal

NATURE CHEMISTRY

A biomimetic molecule liga

Claudio Aquino, Moh
Glenn C. Micalizio

Affiliations | Contribu

Nature Chemistry **4**, 9
Received 21 June 2011

Highlighting tool
Compounds

Abstract

Abstract · Main · Results
Supplementary informati

The discovery of new
protein function often e
is widely recognized th
protein ligands. Much e
like' libraries, yet the sy
by one or more of the f
conformational heterog
infrastructure of moder
describe the design an
merging principles assc
structure of polyketide-
conformationally constr
which offers compatibil
demonstrate that a COF
identifying a non-covale

Subject terms: Cher

NATURE CHEMISTRY DOI: 10.1038/NCHEM.1200 ARTICLES

COPA tetramer
Peptoid tetramer
Peptoid octamer

RRRR
RRSS
RSRS
RSSR

= 2 conformations within 1.1 kcal of low energy conformation
= 7 conformations within 1.1 kcal of low energy conformation
= 13 conformations within 1.1 kcal of low energy conformation

Figure 2 | Stereochemistry of the COPA backbone is anticipated to have a substantial impact on skeletal shape and the disposition of side chains in space. Distribution of conformers found within 1.1 kcal mol^{-1} of the lowest-energy conformation identified. Calculations were conducted with Spartan-08/MMFF model/Conformer Distribution option/Monte Carlo algorithm. Coloured spheres highlight the relative position of heteroatoms (green) and alkenes (blue). Although these molecular mechanics calculations are not interpreted to predict the solution-phase structure of these oligomers, the calculations provide a uniform lens through which to observe unique characteristics associated with this new class of synthetic oligomer.

double asymmetric relationships between amine **11** and acid **1** have little impact on chemical efficiency for this bond construction—a critically important virtue of this chemistry, as split-and-pool techniques will aim to prepare all combinations of stereochemistry along the growing COPA backbone. With regard to this later consideration associated with the projected application of this chemistry in split-and-pool format, we recognize that oligomerization of chiral monomers of 90% e.e. will result in the production of minor diastereomers on each bead. The combinatorial nature of this process, however, will ensure that the population contains beads that present these minor impurities as major constituents. In this way, a built-in control mechanism exists to aid in the analysis of assay results, as the minor component on any particular bead will be present as a major component on a different bead within the collection. That said, we anticipate that conditions can be found in future studies to crystallize intermediate **7** or **8** as a means to attain isomeric homogeneity.

Establishing the value of COPA libraries as a source of protein ligands. Moving forward to explore the utility of COPA oligomers as a potential source of protein ligands, a library of tetramers was prepared by split-and-pool methods. To be compatible with our on-bead screening platform[31], we selected 160 μm TentaGel beads functionalized with a tetrameric polyamide (Fig. 3e), the structure of which was selected to optimize subsequent MS-based structure elucidation (see Supplementary Information for details). Targeting a library of 160,000 members, we used ten primary amines and two pentenoic acids as depicted in Fig. 3d. As we planned to carry out structural elucidation by MS, we used a heavy atom label (CD_3 at C2) to correlate differences in the mass of fragment ions with absolute stereochemistry of the chloropentenoic acid monomer. Alongside these efforts, a library of peptoid tetramers was prepared with the same amines used for the COPA library (Fig. 3f) in an effort to establish a baseline for comparison between these two synthetic oligomer platforms. Matrix assisted laser desorption ionization (MALDI) mass spectra revealed a single strong peak for the COPAs released from several individual beads chosen randomly from the library, indicating that each bead predominantly displays a single compound and that each synthetic step proceeded in high yield.

Having established that the library was of high quality, it was screened against the DNA-binding domain of p53, an important transcription factor that regulates a variety of genes involved in cell cycle control and apoptosis. More than half of human cancers express inactive p53 due to the presence of missense mutations in the DNA-binding domain (DBD) that destabilize the folding of the protein[32]. There is considerable interest in the identification of 'chemical chaperones' whose binding to p53 might stabilize the wild-type, functional, folded conformation[33]. Because transcription factors are generally considered to be extremely challenging targets for small molecules[34], we considered p53 recognition a stringent test of the utility of this new class of compounds.

Purified, bacterially expressed, FLAG-tagged p53–DBD (10 μM) was incubated with the bead-displayed COPA library in the presence of high levels of competitor proteins to suppress non-specific binding events. The beads were then washed and treated with anti-FLAG antibody followed, after another washing step, by anti-IgG antibodies conjugated to red quantum dots. The beads were then examined under a low-power fluorescent microscope. Several beads with a strong red halo surrounding them, indicating binding of the quantum dot via the p53–FLAG/anti-FLAG antibody/anti-IgG–quantum dot sandwich complex, were observed (Fig. 4a). These, as well as some beads with weaker staining, were picked using a micropipette. In all, 22 beads were collected. Six of

NATURE CHEMISTRY | VOL 4 | FEBRUARY 2012 | www.nature.com/naturechemistry 101

elcome back: Jason Wilde
Logout
Go Advanced search
us article next article
scribe
rt sign up
SS feed
olecule library for drug
mbine the favourable
ct structures with the
nthesis.
Continue
View all
ejobs
(W1 / W2)
ter of Excellence
iate Professor of
ns

Beyond [the] paper

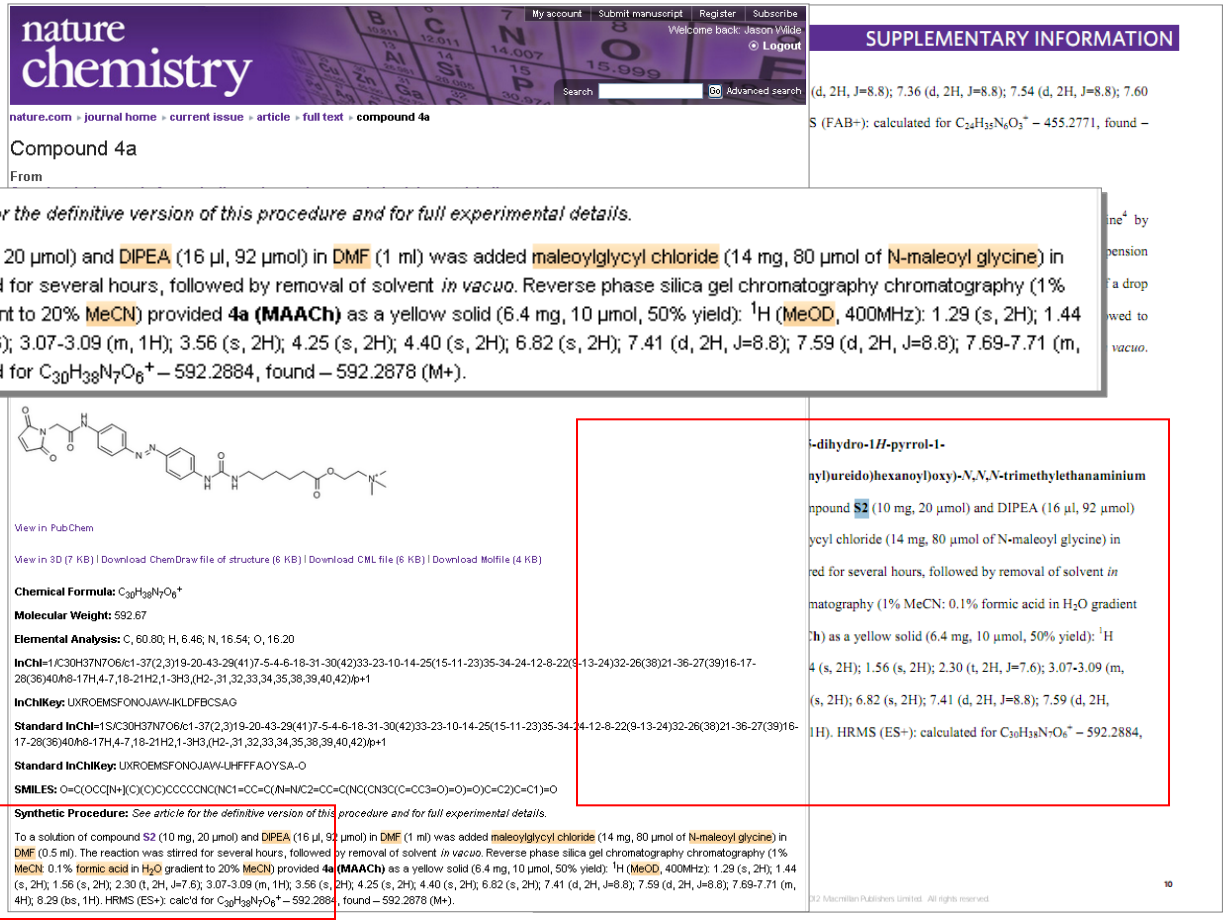

nature chemistry

My account | Submit manuscript | Register | Subscribe

Welcome back: Jason Wilde

Logout

Search | Advanced search

nature.com » journal home » current issue » article » full text » compound 4a

Compound 4a

From

Synthetic Procedure: *See article for the definitive version of this procedure and for full experimental details.*

To a solution of compound S2 (10 mg, 20 µmol) and DIPEA (16 µl, 92 µmol) in DMF (1 ml) was added maleoylglycyl chloride (14 mg, 80 µmol of N-maleoyl glycine) in DMF (0.5 ml). The reaction was stirred for several hours, followed by removal of solvent *in vacuo*. Reverse phase silica gel chromatography chromatography (1% MeCN: 0.1% formic acid in H_2O gradient to 20% MeCN) provided **4a (MAACh)** as a yellow solid (6.4 mg, 10 µmol, 50% yield): ^{1}H (MeOD, 400MHz): 1.29 (s, 2H); 1.44 (s, 2H); 1.56 (s, 2H); 2.30 (t, 2H, J=7.6); 3.07-3.09 (m, 1H); 3.56 (s, 2H); 4.25 (s, 2H); 4.40 (s, 2H); 6.82 (s, 2H); 7.41 (d, 2H, J=8.8); 7.59 (d, 2H, J=8.8); 7.69-7.71 (m, 4H); 8.29 (bs, 1H). HRMS (ES+): calc'd for $C_{30}H_{38}N_7O_6^+$ – 592.2884, found – 592.2878 (M+).

View in PubChem

View in 3D (7 KB) | Download ChemDraw file of structure (6 KB) | Download CML file (6 KB) | Download Molfile (4 KB)

Chemical Formula: $C_{30}H_{38}N_7O_6^+$

Molecular Weight: 592.67

Elemental Analysis: C, 60.80; H, 6.46; N, 16.54; O, 16.20

InChI=1/C30H37N7O6/c1-37(2,3)19-20-43-29(41)7-5-4-6-18-31-30(42)33-23-10-14-25(15-11-23)35-34-24-12-8-22(9-13-24)32-26(38)21-36-27(39)16-17-28(36)40/h8-17H,4-7,18-21H2,1-3H3,(H2-,31,32,33,34,35,38,39,40,42)/p+1

InChIKey: UXROEMSFONOJAW-IKLDFBCSAG

Standard InChI=1S/C30H37N7O6/c1-37(2,3)19-20-43-29(41)7-5-4-6-18-31-30(42)33-23-10-14-25(15-11-23)35-34-24-12-8-22(9-13-24)32-26(38)21-36-27(39)16-17-28(36)40/h8-17H,4-7,18-21H2,1-3H3,(H2-,31,32,33,34,35,38,39,40,42)/p+1

Standard InChIKey: UXROEMSFONOJAW-UHFFFAOYSA-O

SMILES: O=C(OCC[N+](C)(C)C)CCCCCNC(NC1=CC=C(/N=N/C2=CC=C(NC(CN3C(C=CC3=O)=O)=O)C=C2)C=C1)=O

Synthetic Procedure: *See article for the definitive version of this procedure and for full experimental details.*

To a solution of compound S2 (10 mg, 20 µmol) and DIPEA (16 µl, 92 µmol) in DMF (1 ml) was added maleoylglycyl chloride (14 mg, 80 µmol of N-maleoyl glycine) in DMF (0.5 ml). The reaction was stirred for several hours, followed by removal of solvent *in vacuo*. Reverse phase silica gel chromatography chromatography (1% MeCN: 0.1% formic acid in H_2O gradient to 20% MeCN) provided **4a (MAACh)** as a yellow solid (6.4 mg, 10 µmol, 50% yield): ^{1}H (MeOD, 400MHz): 1.29 (s, 2H); 1.44 (s, 2H); 1.56 (s, 2H); 2.30 (t, 2H, J=7.6); 3.07-3.09 (m, 1H); 3.56 (s, 2H); 4.25 (s, 2H); 4.40 (s, 2H); 6.82 (s, 2H); 7.41 (d, 2H, J=8.8); 7.59 (d, 2H, J=8.8); 7.69-7.71 (m, 4H); 8.29 (bs, 1H). HRMS (ES+): calc'd for $C_{30}H_{38}N_7O_6^+$ – 592.2884, found – 592.2878 (M+).

SUPPLEMENTARY INFORMATION

(d, 2H, J=8.8); 7.36 (d, 2H, J=8.8); 7.54 (d, 2H, J=8.8); 7.60

S (FAB+): calculated for $C_{24}H_{35}N_6O_3^+$ – 455.2771, found –

ne[4] by

pension

a drop

wed to

vacuo.

-dihydro-1*H*-pyrrol-1-

nyl)ureido)hexanoyl)oxy)-*N*,*N*,*N*-trimethylethanaminium

npound S2 (10 mg, 20 µmol) and DIPEA (16 µl, 92 µmol)

ycyl chloride (14 mg, 80 µmol of N-maleoyl glycine) in

red for several hours, followed by removal of solvent *in*

matography (1% MeCN: 0.1% formic acid in H_2O gradient

h) as a yellow solid (6.4 mg, 10 µmol, 50% yield): ^{1}H

4 (s, 2H); 1.56 (s, 2H); 2.30 (t, 2H, J=7.6); 3.07-3.09 (m,

(s, 2H); 6.82 (s, 2H); 7.41 (d, 2H, J=8.8); 7.59 (d, 2H,

1H). HRMS (ES+): calculated for $C_{30}H_{38}N_7O_6^+$ – 592.2884,

10

External data/information

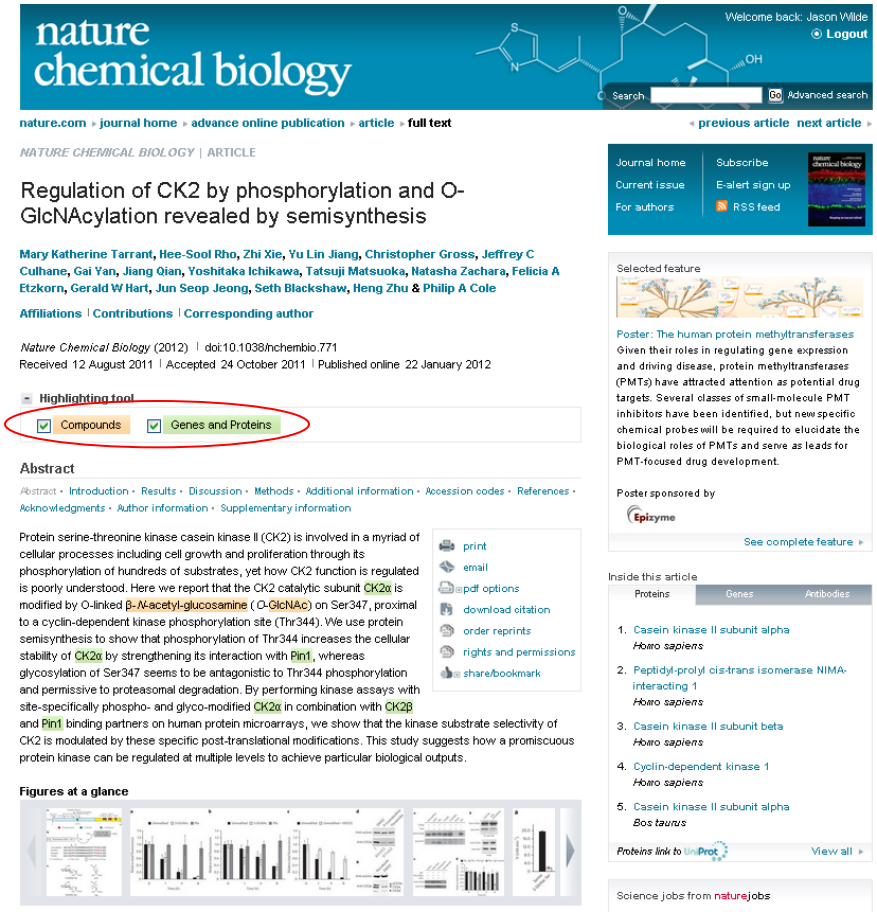

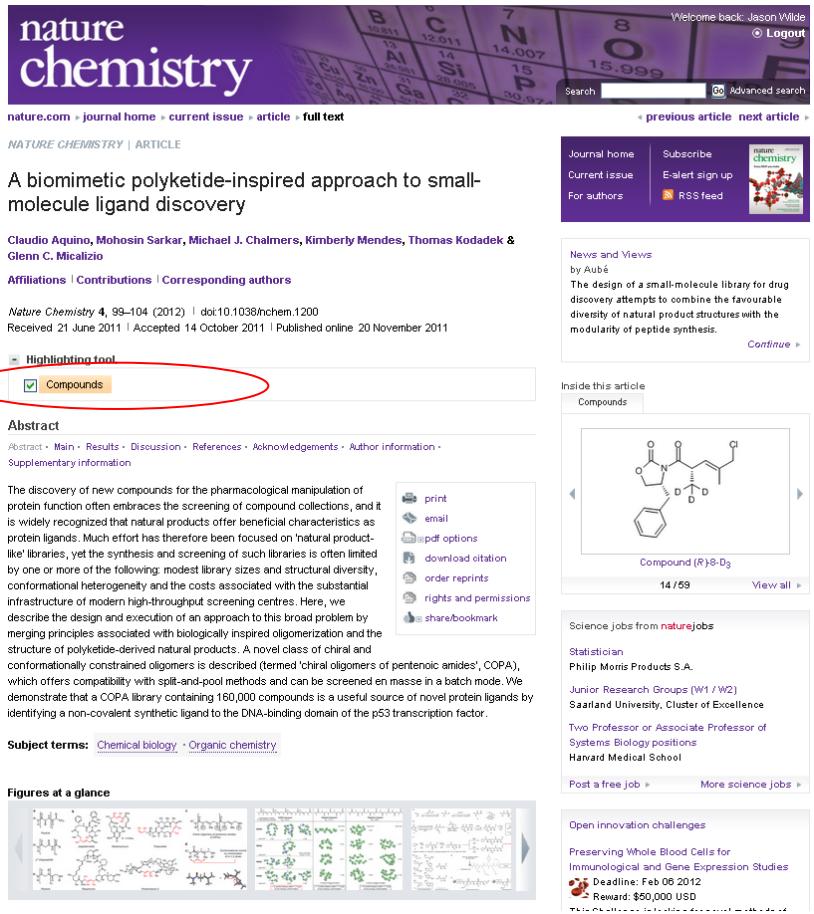

External data/information

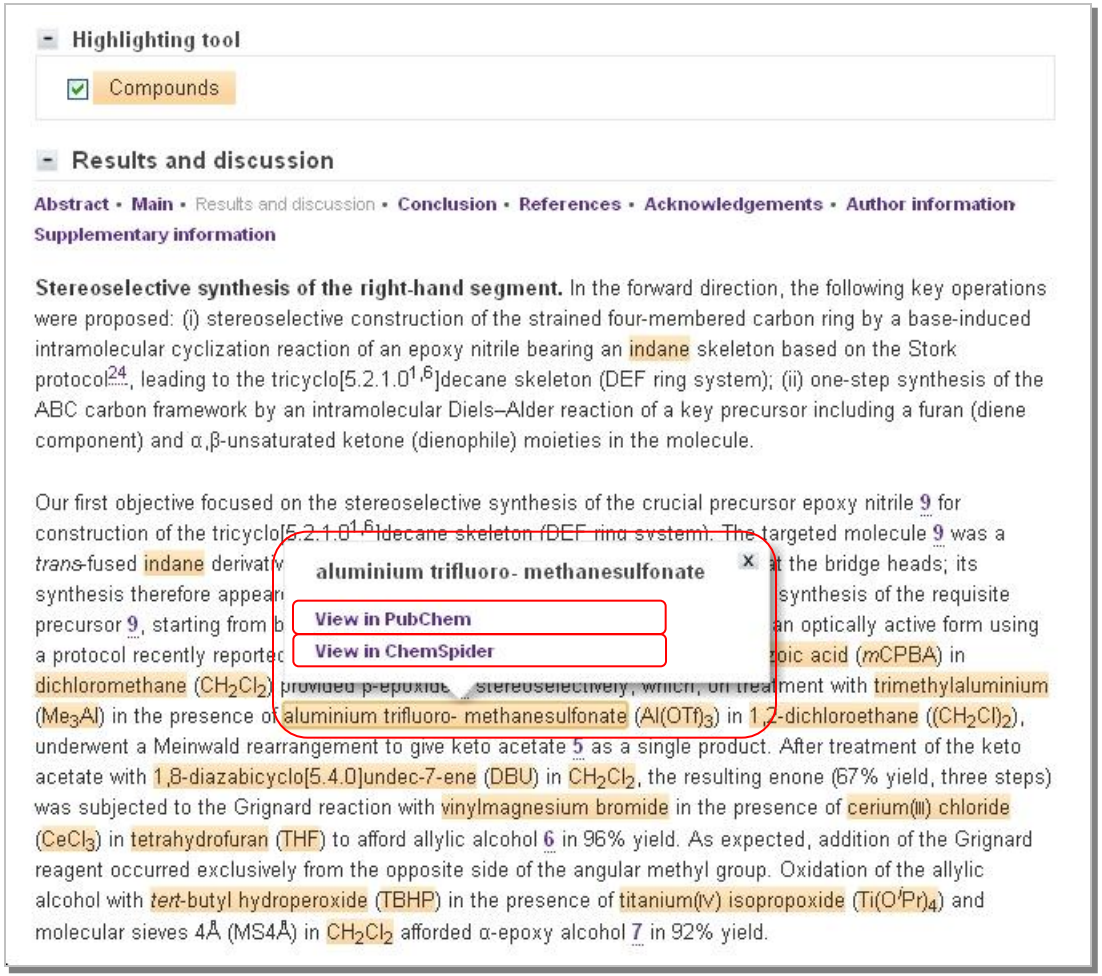

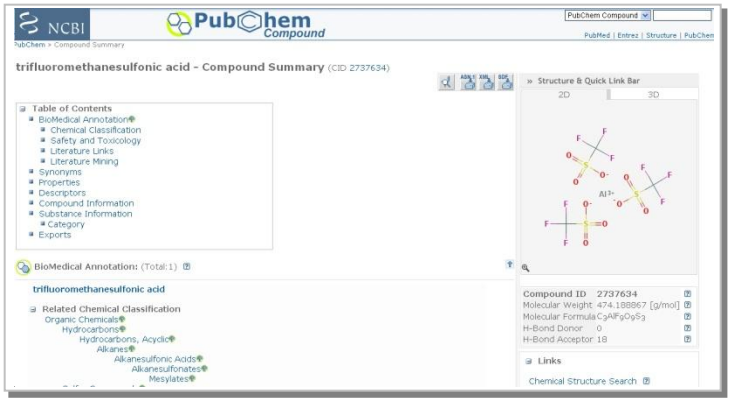

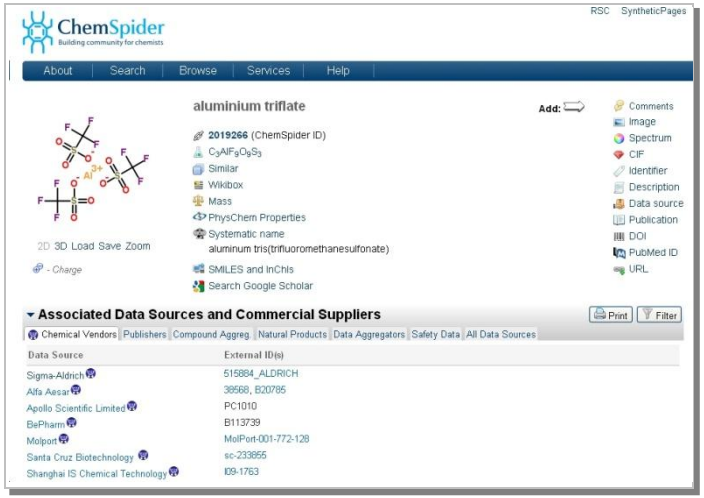

External data/information

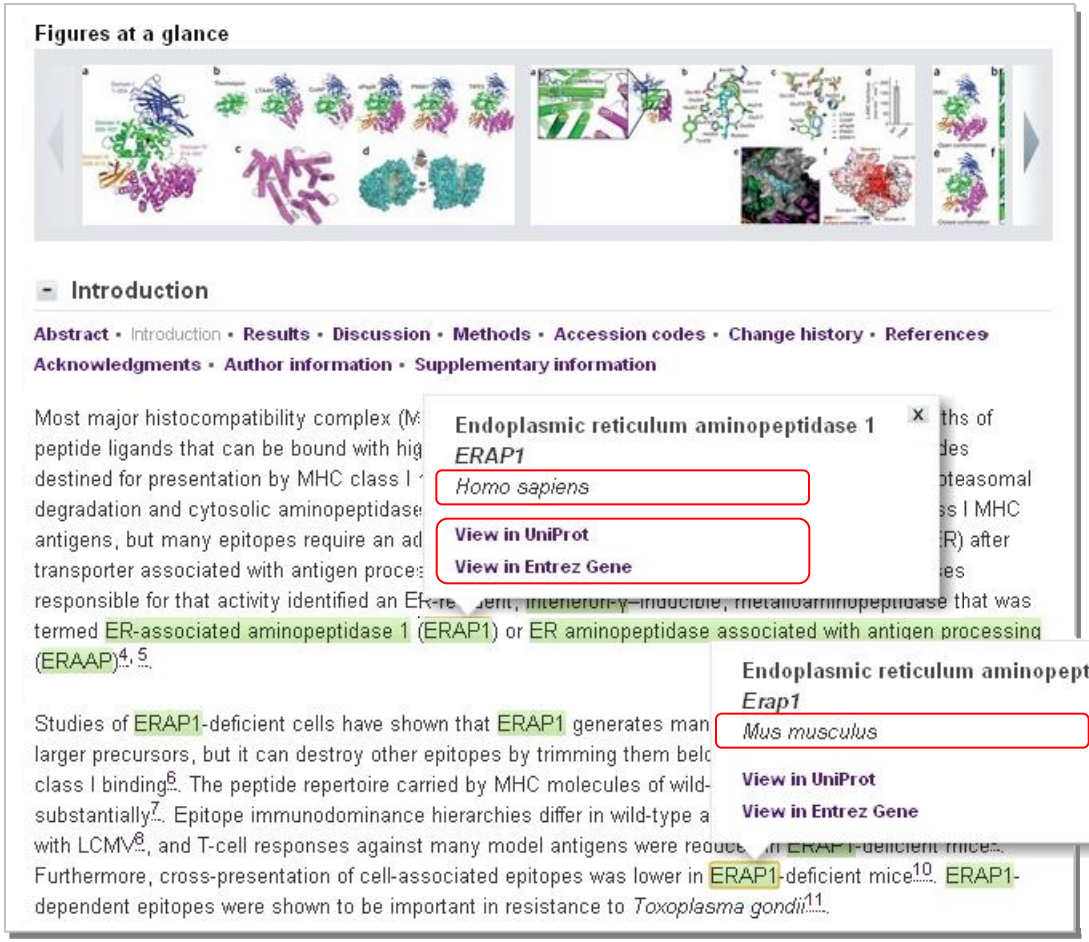

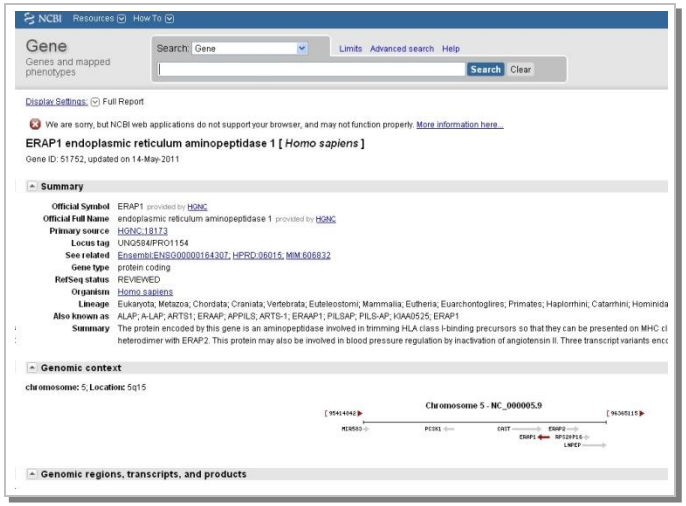

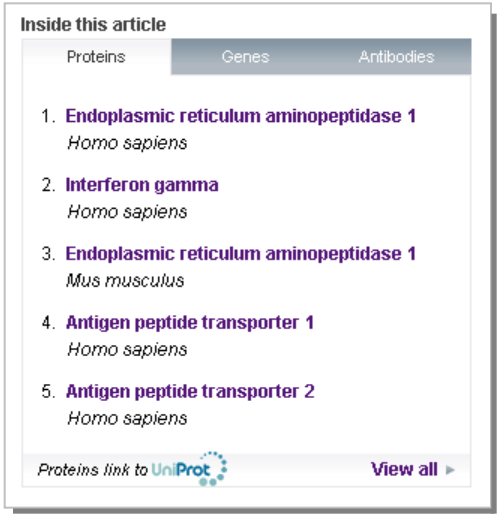

Text, data, metadata…

Authors

Article level metrics

Updates (corrections)

Comments

Social media

Related content & editorial perspective

Sections

Figures

Data & Accession codes

Molecular entities:
- Compounds
- Genes
- Proteins
- Techniques

videos

visualisation tools:
- 3D structure
- Genome browser
- Open microscopy
- environment

blogs
Text, video
podcast

The article of the future..?

Contextual advertising

Patents

Related data files

Faceted sear

ases

Articles about the same entity

New sources of relevant information

endors & Suppliers

Articles need to r nto a 3D entity in the information space.

The article of the future..?

The end..?

- Everything mentioned applies to patents and, more importantly, patents are potentially ‘shouting’ for this more than research articles
- Linking the research to patent literature and the data behind the research is becoming more important
- We (NPG) are seeing a slow (but steady) transition to mobile devices/reading. The driver will be the range of mobile devices and the services/applications they offer

- This is not a short term game – things will evolve over time!
- EXPERIMENT – not one size will ever fit all
- But don’t lose sight of who you are developing for…
  - "Trust me - if you gave people at Google free rein to produce TV you'd end up with a lot of bad sci-fi,"

- What ever happens this is a very exciting time to be developing an exciting medium